DEVELOPMENT OF THE NONLINEAR ENERGY METHOD FOR FRACTURE TOUGHNESS DETERMINATION

D. L. Jones, J. D. Lee and H. Liebowitz

School of Engineering and Applied Science,
The George Washington University,
Washington, D.C. 20052 USA

ABSTRACT

This paper presents a summary of the development of the nonlinear energy ($\tilde{G}$) method for fracture toughness determination that has been pursued at GWU over the last ten years. Although considerable research has been performed in other aspects of fracture mechanics, such as biaxial loading, temperature effects and fatigue; this paper emphasizes static, uniaxial loading on center-cracked and compact tension geometries. The analytical foundation of the method and procedures for evaluating $\tilde{G}$ by the finite-element method are presented, with a major finding being that the plastic energy and crack size are linearly related during subcritical crack growth. Experimental evaluations of $\tilde{G}$ are also presented and comparisons between the finite-element and experimental results are shown to be excellent.

KEYWORDS

Fracture toughness, nonlinear, crack growth, finite-element evaluations, experimental evaluations, comparisons.

INTRODUCTION

Continuing research into fracture mechanics concepts after the acceptance of the standard method for fracture toughness testing of metallic materials, ASTM E399, has led to widespread emphasis on the development of materials having considerably higher fracture toughnesses, while maintaining other properties such as yield strength, etc. The success of these efforts has led to the necessity of employing ever-increasing specimen sizes and testing expenses or the development of new fracture criteria capable of incorporating crack-tip plasticity and subcritical crack growth into the fracture toughness. A number of methods for fracture toughness determination under inelastic (nonlinear) conditions have been proposed including the R-curve, J-integral, crack-opening displacement (COD) and nonlinear energy ($\tilde{G}$) methods.

The nonlinear energy method has been subjected to analytical, finite-element, and experimental development at GWU over the last ten years. Comparisons have been made between $\tilde{G}$ obtained by the finite-element and experimental methods and also with other fracture toughness parameters. The purpose of this paper will be to present: (*i*) the major analytical, finite-element, and experimental developments of the nonlinear energy method, (*ii*) correlations between them, and (*iii*) comparisons with other nonlinear fracture toughness test methods.

ANALYTICAL BACKGROUND

Consider an elastic, (linear or nonlinear) material body, which contains a single crack and is subjected to static loading at the outer boundary. The strains are assumed to be infinitesimal and the elastic material response requires that there exist a strain energy density, ϕ, which is a function of strain only, such that the increment of strain energy of the body, dU, may be written

$$dU \equiv \int_V (d\phi)\, dv = \int_V (\sigma_{ij} de_{ij})\, dv \quad , \text{ where } \sigma_{ij} = \frac{\partial \phi}{\partial e_{ij}} \quad . \tag{1}$$

It is noted that

$$dU = \int_V (\sigma_{ij} du_{i,j})\, dv = \int_V [(\sigma_{ij} du_i)_{,j}]\, dv = \oint (\sigma_{ij} n_j du_i)\, ds \equiv dW \quad , \tag{2}$$

which means that the increment of strain energy over the body equals the increment of work done on the surface of the body. In the previous derivation, the Green-Gauss theorem, which converts the volume integral into a surface integral, and the following equations have been applied

$$e_{ij} = \frac{1}{2}(u_{i,j} + u_{j,i}), \qquad \sigma_{ij} = \sigma_{ji}, \qquad \sigma_{ij,j} = 0 \quad . \tag{3}$$

In the case of no subcritical crack growth, the crack surface does not contribute to the increment of work done, dW, and, therefore, Eq. (2) means that at any point prior to unstable fracture the strain energy of the body is equal to the total work done by the externally applied loading. For a center-cracked specimen subjected to uniaxial loading, as shown in Fig. 1, the work done can be expressed in terms of the load-point displacement, v, as

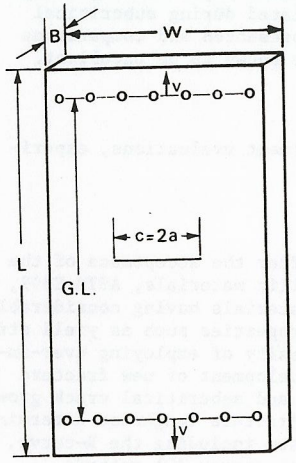

Fig. 1. Specimen Geometry.

$$W = \int_o^V F\, dv \quad , \tag{4}$$

where F is the total applied load. Now, consider a specimen with initial crack size a_1 which is loaded to a certain point A ($F = F_1$, $v = v_1$) and then the crack size is increased to a_2, under: (*a*) fixed load conditions (Fig. 2a), (*b*) fixed grip conditions (Fig. 2b), or (*c*) general conditions (Fig. 2c), along the path AB. The conditions illustrated in Fig. 2 will clearly be different from the situation in which a specimen with initial crack size a_2 is loaded to point B, where the loading path in the load-displacement diagram will be the curve ONB. The increment of external work done between points A and B, dW_{AB}, and the strain energies at points A and B, U_A and U_B, for fixed load, fixed grip, and general conditions can be obtained graphically as:

(*a*) Fixed load conditions; A (F_1, v_1), B (F_1, v_2) ,

$$dW_{AB} = \int_{v_1}^{v_2} F_1 dv = F_1(v_2 - v_1) = \text{Area[ABDCA]} \quad , \tag{5}$$

$$U_A = W_A = \int_o^{v_1} F\, dv = \text{Area[OMACO]}, \quad U_B = W_B = \int_o^{v_2} F\, dv = \text{Area[ONBDO]} \quad . \tag{6}$$

(*b*) Fixed grip conditions; A (F_1, v_1) , B (F_2, v_1) , $dW_{AB} = 0$, (7)

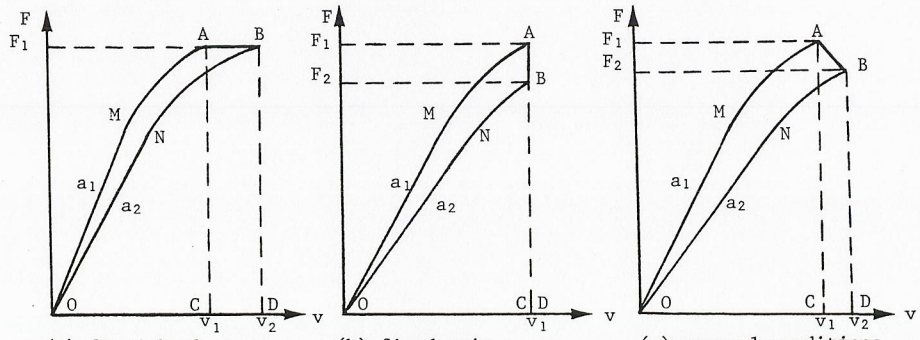

(a) fixed load (b) fixed grip (c) general conditions

Fig. 2. Illustration of fracture under various boundary conditions.

$$U_A = W_A = \int_o^{v_1} F\, dv = \text{Area[OMACO]} \quad , \quad U_B = W_B = \int_o^{v_1} F\, dv = \text{Area[ONBCO]} \quad . \tag{8}$$

(*c*) General conditions; A (F_1, v_1) , B (F_2, v_2) ,

$$dW_{AB} = \int_{v_1}^{v_2} F\, dv = \frac{1}{2}(F_1 + F_2)(v_2 - v_1) = \text{Area[ABDCA]} \quad , \tag{9}$$

$$U_A = W_A = \int_o^{v_1} F\, dv = \text{Area[OMACO]} \quad , \quad U_B = W_B = \int_o^{v_2} F\, dv = \text{Area[ONBDO]}. \tag{10}$$

The energy release rate $\tilde{G}$ is then obtained as

$$\tilde{G} = \lim_{a_2 \to a_1} \left(\frac{dW_{AB} - (U_B - U_A)}{a_2 - a_1} \right) = \lim_{a_2 \to a_1} \left(\frac{\text{Area[OMABNO]}}{a_2 - a_1} \right) \quad . \tag{11}$$

Equation (11) indicates that $\tilde{G}$ is unique irrespective of what conditions were imposed at the onset of unstable fracture.

EVALUATION OF $\tilde{G}_c$ BY THE FINITE-ELEMENT METHOD

From the previous analysis, it is seen that, for the case of no subcritical crack growth, the energy release rate is obtained by differentiating the energy difference between curves OMA, ONB, and line AB with respect to the crack size. Also, it was proved by Lee and Liebowitz (1977) that the energy release rate is obtained by differentiating the complementary energy with respect to the crack size for fixed load conditions or by differentiating the negative of the strain energy with respect to crack size for fixed grip conditions, without the necessity of assuming that the specimen is under uniform uniaxial loading.

Although the expression for $\tilde{G}$, Eq.(11), is only applicable to those cases which have no subcritical crack growth, in almost all practical cases, some subcritical crack growth occurs prior to unstable fracture. To account for the effect of subcritical crack growth, Jones and others (1978) developed four empirical methods for evaluating $\tilde{G}$. According to these four methods, the values of $\tilde{G}$ evaluated by the finite-element method (Lee and Liebowitz, 1978) are 473, 518, 520, 492 (lb/in.) as compared with the experimental values 521, ---, 520, 581 (lb/in.), respectively, for the same specimen. In addition, Lee and Liebowitz (1978) developed a nonlinear finite-element computer program which permits incremental changes in the crack length. This program has two important features. First, it is based on an

incremental theory of plasticity for which the stress-strain relation is expressed in the following incremental forms for loading and unloading,

$$E\,de_{ij} = (1+\nu)\,ds_{ij} + \frac{1-2\nu}{3}\,d\sigma_{kk}\,\delta_{ij} + \frac{3}{2}\,\alpha\sigma_e^{n-1}\,ds_{ij} + \frac{9}{4}\,\alpha\,(n-1)\,\sigma_e^{n-3}\,s_{ij}\,s_{kl}\,ds_{kl} \quad \text{(loading)}, \tag{12}$$

$$E\,de_{ij} = (1+\nu)\,ds_{ij} + \frac{1-2\nu}{3}\,d\sigma_{kk}\,\delta_{ij} \quad \text{(unloading)}. \tag{13}$$

In Eqs. (12) and (13), E is Young's modulus, ν is Poisson's ratio, α and n are material constants and the stress deviator s_{ij}, and the effective stress, σ_e, are defined as

$$s_{ij} \equiv \sigma_{ij} - \frac{1}{3}\,\sigma_{kk}\,\delta_{ij}, \qquad \sigma_e^2 \equiv \frac{3}{2}\,s_{ij}\,s_{ij}. \tag{14}$$

Second, the crack size is regarded as an unknown variable, and therefore a scalar governing equation is needed. At the beginning, the experimental data relating applied load and crack size were taken as the governing equation. Then it was found that, during the entire process of subcritical crack growth, the plastic energy was linearly related to the crack size, i.e.,

$$P - P_i = m\,(a - a_i), \qquad \text{where} \qquad P = \int_A \frac{n}{E\,(n+1)}\,\alpha\sigma_e^{*\,n+1}\,dA. \tag{15}$$

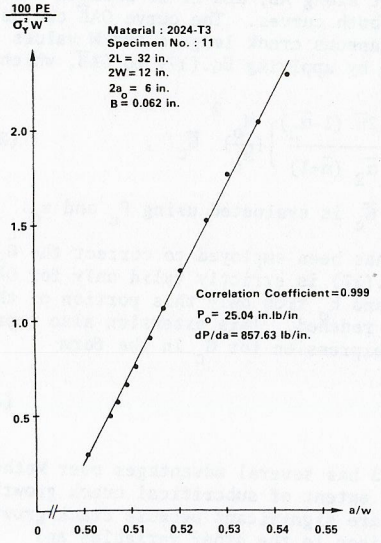

Fig. 3. Linear relation between plastic energy and crack size.

In Eq.(15), σ_e^* is the maximum effective stress, a_i is the initial crack size, and P_i is the critical value of plastic energy beyond which the crack size will be increased. It is noted that the plastic energy, maximum effective stress, and crack size are monotonically increasing quantities during the entire process of subcritical crack growth; and also the irreversible and dissipative nature of plasticity and fracture places considerable significance on the relation exhibited by Eq.(15). For example, a a typical load-crack size curve for a center-cracked 2024-T3 sheet was used to establish the linear relation between plastic energy and crack size, as seen in Fig. 3 (Liebowitz, Lee and Subramonian; 1979a, 1979b). The linear relation was then used as input to the finite-element program (instead of the experimental load-crack size curve) and a computer-generated crack growth resistance curve was seen to fit the experimental data exactly. This procedure has also been successfully applied to other tests on 2024-T3 and 7075-T6 sheets.

Thus, it is possible to use the finite-element program, along with Eq.(15), to evaluate $\tilde{G}$ in the following manner:

(1) Take the experimental load and crack size data (Fig. 4.2), as input to the computer program, and obtain a load-displacement curve (Fig. 4.1) and a linear relation between plastic energy and crack size (Fig. 4.3), which provides the values of P_i and m in Eq.(15). The data for another test are shown in Fig. 5,

and it was found that P_i = 34.14 in.lb/in., and m = 914.04 lb/in.

(2) Take the linear relation between plastic energy and crack size, i.e., line NC in Fig. 4.3, as input with the values of P_i and m obtained previously and the initial crack size to be $a_i' = a_i + \Delta a$. As output, a crack growth resistance curve NC (Fig. 4.2) and a load-displacement curve ONC (Fig. 4.1) are obtained. Notice that, at point C, $a_f' = a_f + \Delta a$.

(3) Although it is noticed that, during the fracture process from point M to point A and from point N to point C, the crack sizes are varying (which is different from the conditions on which Eq.(11) was derived); it is proposed to evaluate $\tilde{G}_c$ in a similar manner, i.e.,

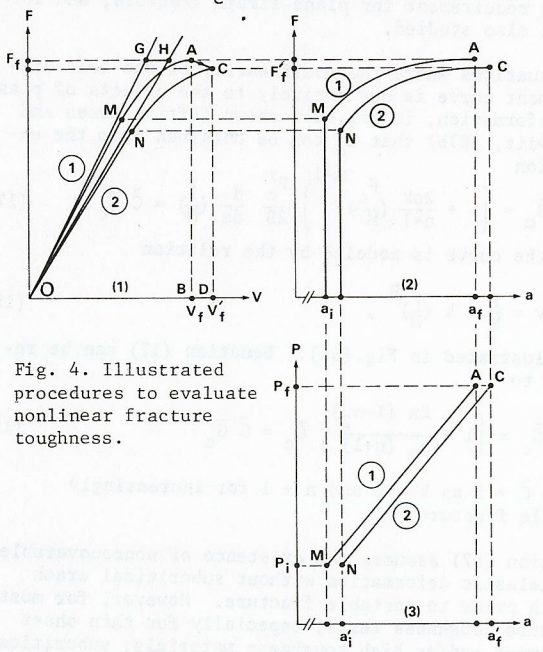

Fig. 4. Illustrated procedures to evaluate nonlinear fracture toughness.

$$\tilde{G}_c = \lim_{a_i' \to a_i} \left(\frac{\text{Area[OMACNO]}}{a_i' - a_i} \right) = \lim_{a_f' \to a_f} \left(\frac{\text{Area[OMACNO]}}{a_f' - a_f} \right). \tag{16}$$

For the data given in Fig. 5, the energy release rate, $\tilde{G}_c$, obtained from Eq.(16) was 654 lb/in. and the experimental value based on the first method proposed by Jones and others (1978), was 646 lb/in., with a difference of 1.14%. In using this proposed method to evaluate the energy release rate, it is not necessary to use the ASTM formula to calculate the stress intensity factor or the G-K relation to obtain the linear energy release rate, $\tilde{G}_c$, nor is it necessary to assume a particular form for the load-displacement curve in order to calculate $\tilde{C}$.

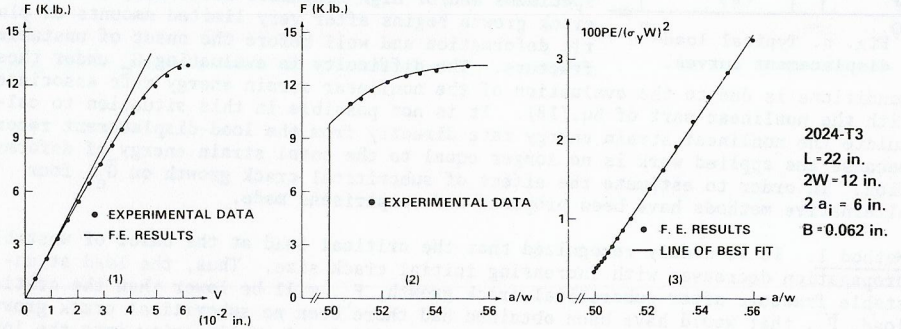

Fig. 5. Relations between applied load, gauge point displacement, crack size, and plastic energy.

EXPERIMENTAL EVALUATION METHODS FOR $\tilde{G}_c$

In order to obtain a careful assessment of the value of the nonlinear energy method as a measure of fracture toughness in the nonlinear range, an experimental program has also been pursued over the last 10 years. This program has encompassed comparisons of center-cracked data of five aluminum alloys and compact-tension tests on two steels, two titanium and several aluminum alloys. For the center-cracked panels, the effect of specimen geometry was examined by conducting test series involving the independent variation of specimen length, width, and crack length-to-width ratio (Jones and others, 1978). In addition, the influence of anti-buckling guides was examined and in most cases comparisons were made with the R-curve method. For the compact tension specimens, test series were performed at various thicknesses above and below the minimum requirement for plane-strain fracture, and for some materials the size effect was also studied.

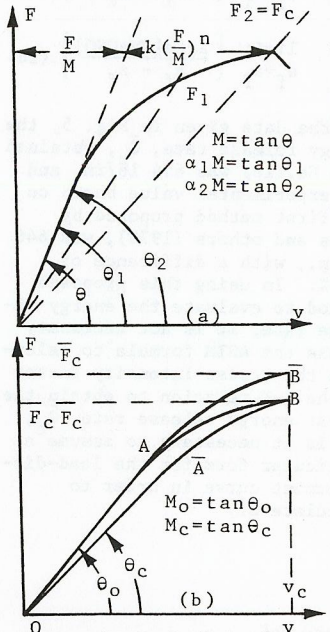

Fig. 6. Typical load-displacement curves.

In situations where the nonlinearity of the load-displacement curve is due entirely to the effects of plastic deformation, it has been shown (Eftis, Jones and Liebowitz, 1975) that $\tilde{G}_c$ can be obtained from the expression

$$\tilde{G}_c = \left(1 + \frac{2nk}{n+1}\left(\frac{F_c}{M}\right)^{n-1}\right)\frac{F_c^2}{2B}\frac{d}{da}\left(\frac{1}{M}\right) = \tilde{C}\,\bar{G}_c \,, \qquad (17)$$

when the curve is modeled by the relation

$$v = \frac{F}{M} + k\left(\frac{F}{M}\right)^n \,, \qquad (18)$$

as illustrated in Fig.(6a). Equation (17) can be reduced to

$$\tilde{G}_c = \left(1 + \frac{2n\,(1-\alpha_2)}{\alpha_2\,(n+1)}\right)\bar{G}_c = \tilde{C}\,\bar{G}_c \qquad (19)$$

where $\tilde{C} \to 1$ as $k \to 0$ and $n \to 1$ for increasingly brittle fracture.

Equation (17) assumes the existence of nonrecoverable or inelastic deformation without subcritical crack growth prior to unstable fracture. However, for most fracture toughness tests, especially for thin sheet specimens and/or high toughness materials, subcritical crack growth begins after very limited amounts of plastic deformation and well before the onset of unstable fracture. The difficulty in evaluating $\tilde{G}_c$ under these conditions is due to the evaluation of the nonlinear strain energy rate associated with the nonlinear part of Eq.(18). It is not possible in this situation to calculate the nonlinear strain energy rate directly from the load-displacement record because the applied work is no longer equal to the total strain energy of deformation. In order to estimate the effect of subcritical crack growth on $\tilde{G}_c$, four alternative methods have been proposed and comparisons made.

Method 1. It is widely recognized that the critical load at the onset of unstable propagation decreases with increasing initial crack size. Thus, the load at unstable fracture after subcritical crack growth, F_c, will be lower than the critical load, $\bar{F}_c$, that would have been obtained had there been no subcritical crack growth. However, subcritical crack growth introduces additional nonlinearity into the load-displacement record, thus increasing $\tilde{C}$ relative to the situation with no subcritical crack growth. Therefore, the effects of subcritical crack growth on F_c and $\tilde{C}$ tend to offset each other in their effect on $\tilde{G}_c$, which suggests that one method of incorportating subcritical crack growth into $\tilde{G}_c$ would be to use the actual load-displacement curve (including crack growth) to determine $\tilde{C}$ and F_c, and the initial crack size to determine $\bar{G}_c$. Determination of $\tilde{G}_c$ values for center-cracked panels by Method 1 thus involves the use of the initial crack size, a_o, and the actual load-displacement record to determine $\tilde{C}$ and F_c. These quantities are then incorporated into Eqs.(17) or (19), where $\bar{G}_c$ is obtained from the appropriate stress intensity factor and G-K relation. For the center-cracked geometry, Eq.(19) becomes

$$\tilde{G}_c = \left(1 + \frac{2n\,(1-\alpha_2)}{\alpha_2\,(n+1)}\right)\left(\frac{F_c}{wB}\right)^2\frac{\pi a_o}{2E}\left(1 - 0.1\left(\frac{a_o}{w}\right) + \left(\frac{a_o}{w}\right)^2\right)^2 . \qquad (20)$$

Method 2. A typical load-displacement record incorporating subcritical crack growth is shown as OAB in Fig. 6b, where the slope of the linear portion of the curve, M_o, is considered to be a function of the crack size only. If subcritical crack growth had not occurred, the path would have followed OA$\bar{B}$ instead. A correction to the crack growth portion (AB) of the curve to account for subcritical crack growth can be introduced in the following manner. At any point along AB, the crack length is $a > a_o$, the displacement is v and the applied load is F. Without subcritical crack growth, the load $\bar{F}$ will always be greater than the actual applied load by the amount

$$\bar{F} = F\,\frac{M_o}{M} \quad \text{and, at unstable fracture,} \quad \bar{F}_2 = F_c\,\frac{M_o}{M_c} \qquad (21a,b)$$

where 1/M represents the compliance at any point along AB, and it is assumed that the critical displacement, v_c, is the same for both curves. The curve OA$\bar{B}$ can be constructed from Eq.(21a) by use of the instantaneous crack lengths and M values along AB. An evaluation of $\tilde{G}_c$ can then be made by applying Eq.(17) to OA$\bar{B}$, which yields

$$\tilde{G}_{c_{..}} = \left(1 + \frac{2\bar{n}\,(1-\bar{\alpha}_2)}{\bar{\alpha}_2\,(\bar{n}+1)}\right)\frac{\bar{F}_c^{\,2}}{2B}\frac{d}{da}(1/M_o) = \left(1 + \frac{2\bar{n}\,(1-\bar{\alpha}_2)}{\bar{\alpha}_2\,(\bar{n}+1)}\right)\left(\frac{M_o}{M_c}\right)^2\bar{G}_c \,, \qquad (22)$$

where the bar over n and α_2 refers to OA$\bar{B}$, and $\bar{G}_c$ is evaluated using F_c and a_o.

Method 3. Another method similar to Method 2 has been employed to correct the $\tilde{G}_c$ values for subcritical crack growth. Since Eq.(17) is strictly valid only for OA in Fig. 6b, Method 3 employs values of M_o, n_o and k_o from only this portion of the curve and extends OA using Eq.(18) until v_c is reached. This extension also represents a curve of the type OA$\bar{B}$ and leads to an expression for $\tilde{G}_c$ in the form

$$\tilde{G}_c = \left(1 + \frac{2n_o\,(1-\alpha_2)}{\alpha_2\,(n_o+1)}\right)\bar{G}_o \,, \qquad (23)$$

where $\bar{G}_o$ is evaluated from $\bar{F}_c$ and a_o. Method 3 has several advantages over Method 2 since there is no need to determine M or the extent of subcritical crack growth at various points along AB. These advantages are significant because crack growth measurement is relatively inaccurate in comparison to the other variables and usually require additional specimens and test measurements.

Method 4. This method is based on use of the critical crack size to obtain a modified load-displacement record, O$\bar{A}\bar{B}$ in Fig. 6b. This curve is obtained by assuming the initial crack size to be a_c and employing n_o and k_o as defined in Method 3. The nonlinear energy fracture toughness can then be obtained from

$$\tilde{G}_c = \left(1 + \frac{2n_o\,(1-\alpha_2)}{\alpha_2\,(n_o+1)}\right)\left(\frac{F_c}{wB}\right)^2 \frac{\pi a_c}{2E}\left(1 - 0.1\,\frac{a_c}{w} + \left(\frac{a_c}{w}\right)^2\right)^2 \qquad (24)$$

for the center-cracked geometry. Method 4 has the advantage that it is not necessary to make assumptions about the critical displacement, v_c, but shares with Method 2 the necessity of determining the critical crack size.

EXPERIMENTAL RESULTS

The first results to be reported in this section will be some comparisons between the four methods just discussed. All four methods have been applied to two center-cracked sheets of 2024-T3 aluminum and the resulting toughness values are shown in Table 1. These comparisons show that there is a variation of approximately 12% in $\tilde{C}$ and 17% in $\bar{G}_c$ for each of the two tests. However, the compensating nature of these variations is clearly seen in the results for $\tilde{G}_c$ which vary less than 8% for both tests. It is noted that the Method 1 fracture toughness values are the smallest of the four methods and thus represent a slightly more conservative estimate

TABLE 1 $\tilde{G}_c$ Values Obtained by Four Methods of Crack Growth Correction For Two 2024-T3 Specimens

Specimen No.	Method of calculation	$\tilde{C}$	$\tilde{G}_c$ (lb/in.)	$\tilde{G}_c$ (MJ/M^2)	$\bar{G}_c$ (lb/in.)	$\bar{G}_c$ (MJ/m^2)
1	1	1.422	394	0.0690	560	0.0981
1	2	1.258	465	0.0814	585	0.1025
1	3	1.332	427	0.0747	569	0.0996
1	4	1.332	455	0.0796	606	0.1061
2	1	1.318	401	0.0702	529	0.0926
2	2	1.164	467	0.0817	543	0.0951
2	3	1.209	448	0.0784	541	0.0947
2	4	1.209	470	0.0824	569	0.0996

of $\tilde{G}_c$ than the other three. These results, and a number of other comparisons giving similar results (Jones and others, 1978), have led to the conclusion that Method 1 is the preferred alternative since it is the most easily used and the others provide differences less than the normal experimental scatter encountered in fracture toughness testing. The remainder of this section will present a number of $\tilde{G}_c$ evaluations, all based on Method 1, and some comparisons with other nonlinear fracture toughness parameters.

Center-cracked panel tests. A large number of fracture toughness tests have been performed on several aluminum alloys 7075-T6, 2014-T6, 2024-T3, 2024-T81 and 7475-T61. The effects of variations in all of the geometric variables, including length, width, and crack length-to-width ratio have been examined. Because of the interest in the effect of subcritical crack growth on fracture toughness values the toughness values were evaluated at both the onset of subcritical crack growth, $\tilde{G}_o$, and at unstable fracture, $\tilde{G}_c$. The linear toughness parameter, $\bar{G}_o$, was also evaluated at the initiation of subcritical crack growth to provide baseline data. Because of space limitations, only one test series, which is generally typical of the results, will be presented. Figure 7 shows the results of the test series on 2024-T3 in which the gauge length was varied. The fracture toughness values, $\tilde{G}_o$ and $\bar{G}_o$, evaluated at the onset of subcritical crack growth are both nearly equal and independent of gauge length (and specimen length as indicated in Fig. 1). However, when the fracture toughness is evaluated at the onset of unstable fracture, using Method 1, the toughness values are no longer independent of gauge length. Also they become

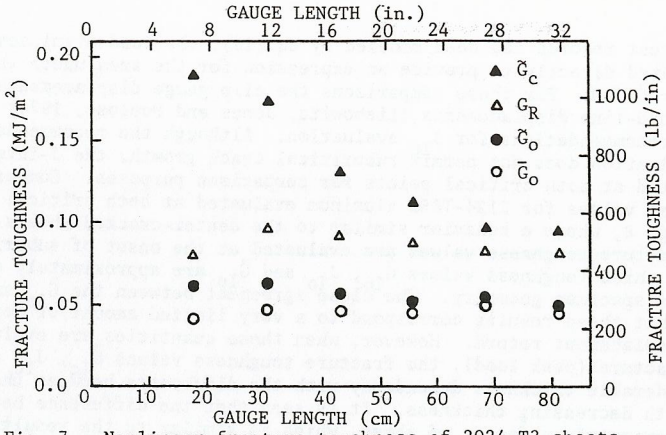

Fig. 7. Nonlinear fracture toughness of 2024-T3 sheets.

much larger than $\tilde{G}_o$ for the shortest specimens.

Compact tension tests. In order to obtain more information about the characteristics of the nonlinear energy method, a number of additional fracture toughness tests have been performed on 7075-T651, 2048-T351, 2048-T851, 2124-T851, and 7175-T7651 aluminum alloys, 4340 and A533B steels, and Ti-6Al-4V and Corona 5 titanium alloys. The specimen dimensions corresponded to ASTM E399 except for the thickness which varied from above to well below the minimum value for plane strain fracture toughness determination. The provisions of E399 were followed insofar as they were applicable to these tests, with the principal exceptions that $\tilde{G}_{Ic}$ and $\tilde{G}_{Io}$ were used to designate all toughness values regardless of specimen thickness and the fracture toughness values were evaluated at both the initiation of subcritical crack growth and at unstable fracture. For most of these tests, comparisons were also made with the J-integral toughness obtained from the formula $J_{Ic} = 2A/Bb$, where A is the area under the load-displacement record and b is the remaining ligament length. Since

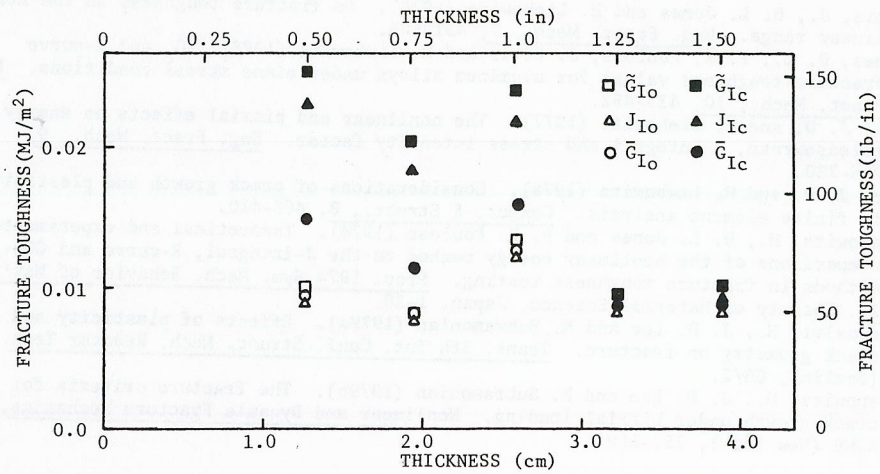

Fig. 8. Variation of toughness parameters with thickness for 2124-T851(T-L).

all of the test records had been modeled by Eq.(18), the load-displacement records were integrated directly to provide an expression for the area under the curve in the form $A = \tilde{C}F/2M$. For these comparisons the clip gauge displacements were converted to load-line displacements (Liebowitz, Jones and Poulose, 1974) in accordance with recommendations for J_{Ic} evaluation. Although the recommended practice for J_{Ic} evaluation does not permit subcritical crack growth, the J-integral was also evaluated at both critical points for comparison purposes. Comparisons between the toughness values for 2124-T851 aluminum evaluated at both critical points are shown in Fig. 8, where a behavior similar to the center-cracked sheets is observed. When the fracture toughness values are evaluated at the onset of subcritical crack growth, all three toughness values $\tilde{G}_{Io}$, J_{Io} and $\tilde{G}_{Io}$ are approximately equal and independent of specimen geometry. The close agreement between the $\tilde{G}_{Io}$ and $\bar{G}_{Io}$ values indicates that these results correspond to a very limited amount of nonlinearity in the load-displacement record. However, when these quantities are evaluated at unstable fracture (peak load), the fracture toughness values $\tilde{G}_{Ic}$, J_{Ic} and $\bar{G}_{Ic}$ exhibit considerable thickness dependency with the difference between the values increasing with decreasing thickness. It is seen that the difference between $\tilde{G}_{Ic}$ and $\tilde{G}_{Io}$ is approximately a factor of three, which is similar to the results given for 2024-T3 in Fig. 7. Although many additional test series have been performed, space limitations preclude their inclusion in this paper.

CONCLUSIONS

(1) The nonlinear energy method has been developed as a self-consistent method for fracture toughness determination under elastic-plastic conditions and as an effective approximate method when subcritical crack growth is included.

(2) A procedure for evaluating $\tilde{G}$ by the finite-element method was presented, with a major finding being the linear relation between the plastic energy and the crack size during subcritical crack growth.

(3) Correlations have been made between $\tilde{G}$ evaluated by the finite-element and experimental methods and the agreement between them was excellent.

REFERENCES

Eftis, J., D. L. Jones and H. Liebowitz (1975). On fracture toughness in the nonlinear range. Eng. Fract. Mech., 7, 491-503.

Jones, D. L., P. K. Poulose, J. Eftis and H. Liebowitz (1978). $\tilde{G}_c$ and R-curve fracture toughness values for aluminum alloys under plane stress conditions. Eng. Fract. Mech., 10, 433-452.

Lee, J. D. and H. Liebowitz (1977). The nonlinear and biaxial effects on energy release rate, J-integral and stress intensity factor. Eng. Fract. Mech., 9, 765-780.

Lee, J. D. and H. Liebowitz (1978). Considerations of crack growth and plasticity in finite element analysis. Comput. & Struct., 8, 403-410.

Liebowitz, H., D. L. Jones and P. K. Poulose (1974). Theoretical and experimental comparisons of the nonlinear energy method to the J-integral, R-curve and COD-methods in fracture toughness testing. Proc. 1974 Sym. Mech. Behavior of Mat'ls., 2. Society of Material Science, Japan, 1-20.

Liebowitz, H., J. D. Lee and N. Subramonian (1979a). Effects of plasticity and crack geometry on fracture. Trans. 5th Int. Conf. Struct. Mech. Reactor Tech. (Berlin), G6/2.

Liebowitz, H., J. D. Lee and N. Subramonian (1979b). The fracture criteria for crack growth under biaxial loading. Nonlinear and Dynamic Fracture Mechanics, ASME (New York), 157-169.